arXiv:0812.1522v1 [cond-mat.other] 8 Dec 2008

,

Coherence properties and luminescence spectra of condensed polaritons in CdTe microcavities

M. H. Szymańska,[1] F. M. Marchetti,[2] J. Keeling,[3] and P. B. Littlewood[3]

[1] *Clarendon Laboratory, Department of Physics, University of Oxford, Parks Road, Oxford, OX1 3PU, UK*
[2] *Rudolf Peierls Centre for Theoretical Physics, 1 Keble Road, Oxford OX1 3NP, UK*
[3] *Cavendish Laboratory, University of Cambridge, Madingley Road, Cambridge CB3 0HE, UK*

(Dated: December 8, 2008)

We analyse the spatial and temporal coherence properties of a two-dimensional and finite sized polariton condensate with parameters tailored to the recent experiments which have shown spontaneous and thermal equilibrium polariton condensation in a CdTe microcavity [Kasprzak *et al.*, Nature **443**, 409 (2006)]. We obtain a theoretical estimate of the thermal length, the lengthscale over which full coherence effectively exists (and beyond which power-law decay of correlations in a two-dimensional condensate occurs) of the order of 5μm. In addition, the exponential decay of temporal coherence predicted for a finite size system is consistent with that found in the experiment. From our analysis of the luminescence spectra of the polariton condensate, taking into account pumping and decay, we obtain a dispersionless region at small momenta of the order of 4 degrees. In addition, we determine the polariton linewidth as a function of the pump power. Finally, we discuss how, by increasing the exciton-photon detuning, it is in principle possible to move the threshold for condensation from a region of the phase diagram where polaritons can be described as a weakly interacting Bose gas to a region where instead the composite nature of polaritons becomes important.

PACS numbers: 03.75.Kk, 71.35.Lk, 71.36.+c, 03.75.Gg

I. INTRODUCTION

Since the first observation of polariton bosonic stimulation under non resonant excitation obtained in 1998 in a CdTe microcavity[1], there has been a considerable interest in realising a polariton Bose-Einstein condensate (see, e.g., the recent review[2] and references therein). This search has been mainly motivated by the expected high transition temperature of polaritons due to their very light effective mass[3,4,5]. A spontaneous and thermal equilibrium polariton condensate has been very recently achieved in a CdTe microcavity[6]. This was soon followed by similar effects in a GaAs microcavity[7,8]. Other recent progress in polariton condensation includes studying trapped polaritons in a GaAs structure under stress[9] and room temperature polariton lasing in GaN[10].

The microcavity polariton system is finite, two-dimensional, decaying, and interacting, and therefore is expected to differ from the Bose-Einstein condensation of ideal three-dimensional bosons. Much theoretical work involving different modelling has been done to evaluate the phase diagram for microcavity polaritons[3,4,5,11,12] — for a comprehensive review on the use of and comparison between different models see Ref.[2]. Already the results obtained in[5,12], and adapted to the CdTe experiment[6], have shown a very good agreement between the experimental estimate of the critical density for condensation obtained from the occupation data — at a given temperature and detuning conditions — and the theoretical estimate obtained from the lower polariton blue-shift (see the online supplementary information of Ref.[6]). Recently, a direct comparison between experimental and theoretical phase boundaries for condensation of microcavity polaritons in CdTe under different conditions of cryostat temperature and detuning have been performed in Ref.[13]. In that work, it was shown that for a steady state situation, in the presence of pumping and decay, although the polaritons may display a thermal population, the presence of pumping and decay may yet have noticeable effects. In particular the small discrepancies between the experimental data and the equilibrium theoretical estimates for a closed system can be attributed to the effects of pump and decay.

In fact, it has been already shown[14,15] that quantum condensation is indeed possible in strongly dissipative systems with continuous pump and decay and that it shares several features with quantum condensation in a closed system at equilibrium. In particular, the mechanism of condensation, connected with the chemical potential reaching the lower polariton (LP) mode, is exactly the same in closed systems at equilibrium and in open systems with pump and decay. In the latter, the role of the chemical potential is played by the energy at which the non-thermal distribution diverges. However, it has been shown[14,15] that the presence of pump and decay can significantly modify the coherence properties of the condensate. In particular, the power-law decay of temporal and spatial correlations, caused by the 2D nature of the polariton system, can be strongly modified by the presence of dissipation. Finally, it has been shown[15] that the finite size of the system additionally modifies the temporal coherence properties and in particular it leads to a crossover from a power-law decay of temporal coherence in an infinite system to an exponential decay in a

finite system.

As well as coherence measurements, changes to the photoluminescence spectrum can also provide evidence for quantum condensation. The photoluminescence spectrum reflects the structure of the normal modes of the microcavity system, weighted (in thermal equilibrium) by the bosonic occupation factor. The structure of collective modes changes dramatically when microcavity polaritons condense: The lower and upper polariton modes, which are the eigenmodes of the system in the non-condensed regime, are now replaced by two new eigenmodes. In particular, the lower polariton is replaced by the collective (Goldstone) mode and its quadratic dispersion evolves to a linear dispersion at small momenta in the closed equilibrium system[5,12,16], while it becomes diffusive at small momenta in the open system with pump and decay[14,15,17,18].

In this paper we discuss the consequences of these general results for the properties of coherence and luminescence spectra of microcavity polaritons in the specific conditions of the CdTe experiments[6,13]. In particular, by considering the closed system, we give estimates of the thermal length, the lengthscale over which full coherence effectively exists (and beyond which power-law decay of correlations in a two-dimensional condensate occurs), and find that its value, of the order of 5μm, is consistent with the measurements of the spatial decay of the first order coherence reported in[6]. We also consider effects due to pump and decay, and calculate the luminescence spectra for the conditions of the CdTe experiments and in particular analyse the size of the diffusive region as well as the size of the linear regime in the luminescence. The non-equilibrium formalism, which accounts for the effects of pump and decay, also allows us to calculate the homogeneous polariton linewidth as a function of the pump power. Finally, in Ref.[13] it has been shown that the experimental data for the phase boundary lie close to the crossover region between a Berezhinskii-Kosterlitz-Thouless (BKT) transition of structureless bosons and a regime where instead the boundary is determined by the long-range nature of the polariton-polariton interaction. In this paper we show how the increase of the exciton-photon detuning, which results in a higher transition density at a given temperature, moves the transition (at a given temperature) from the BKT weakly interacting Bose boundary to a regime where the composite nature of polaritons becomes important.

The paper is organised as follows: in Sec II we analyse coherence properties on the basis of an equilibrium theory for a closed system and in Sec. III we discuss how non-equilibrium and finite size effects modify these results. Finally, in Sec. IV we analyse the influence of the exciton-photon detuning on the polariton phase diagram.

II. COHERENCE PROPERTIES AT EQUILIBRIUM

The coherence properties of the condensed polariton system are described by the functional form of the first order coherence as a function of time and space:

$$g^{(1)}(t;\mathbf{r}) = \frac{\langle\psi^\dagger(\mathbf{r},t)\psi(\mathbf{0},0)\rangle}{\sqrt{\langle\psi^\dagger(\mathbf{0},0)\psi(\mathbf{0},0)\rangle\langle\psi^\dagger(\mathbf{r},t)\psi(\mathbf{r},t)\rangle}} \ , \quad (1)$$

where $\psi(\mathbf{r},t)$ is the photon field. To determine the characteristic length- and time-scales in $g^{(1)}(t;\mathbf{r})$, we must therefore evaluate the correlation function in the numerator of Eq. (1), which can be achieved by finding the normal modes — i.e. collective quasi-particle excitations — of the system. We will therefore start our analysis by determining the spectrum of the collective excitations above the polariton condensate, making use of a Bose-Fermi model — tailored to the parameters characterising the CdTe microcavities[6,13] — which takes into account the composite nature of polaritons, the quantum well disorder, and the non-linearities associated with exciton-photon interactions (for more details on the model see Refs.[2,12,19]).

A. Collective modes of the polariton condensate

The spectra of the collective modes of a polariton condensate can be evaluated by considering the second order fluctuations above the mean-field approximation (see, e.g.[5,12,16,19]). One can show that, when the system condenses, the lower and upper polariton modes are not any longer the eigenmodes of the problem and are instead replaced by new collective modes: The lower polariton becomes a linear (Goldstone) mode at low momenta, while two new branches appear below the chemical potential, which are seen as gain in the spectral weight $W(\omega,\mathbf{p})$ (see Fig. 1 — in which the second branch below the chemical potential emitting at around $\omega-\omega_0=-41$meV is not shown). Note that Fig. 1 shows the incoherent emission only, without including the condensate emission. These features in the spectral weight will influence the photoluminescence (PL) emission,

$$P(\omega,\mathbf{p}) = n_B(\omega)W(\omega,\mathbf{p}) \ , \quad (2)$$

which is the product of the spectral weight times the Bose occupation factor $n_B(\omega)$. The observation of these predicted features in the photoluminescence would provide very strong evidence for polariton condensation. However, the emission from below the chemical potential is suppressed at large angles (see[19]), while the PL emission from modes far above the chemical potential is suppressed exponentially by the thermal occupation of these modes, making such features hard to observe. In addition, the strong emission from the condensate at zero momentum and the frequency corresponding to the chemical potential, which is not shown in Fig. 1, might mask

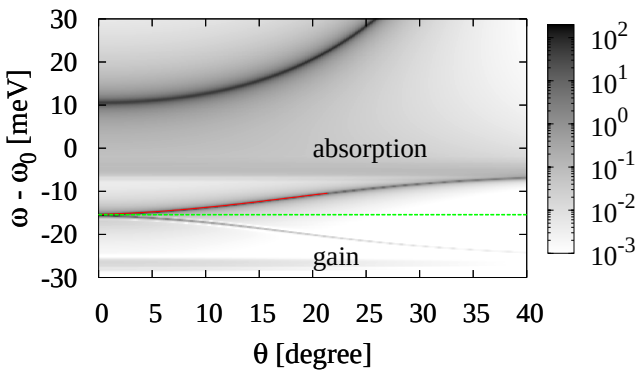

FIG. 1: Contour plot of the spectral weight $W(\omega, \mathbf{p})$ as a function of energy $\omega - \omega_0$, where ω_0 indicates the bare cavity photon energy, and emission angle $\theta = \sin^{-1}(c|\mathbf{p}|/\omega_0)$ for a closed equilibrium system at temperature $T = 19$K, detuning $\delta = +6$ meV and a fixed density $n = 6.1 \times 10^8 \mathrm{cm}^{-2}$ (the mean-field critical density for condensation for these values of temperature and detuning is given by $n_c = 6 \times 10^7 \mathrm{cm}^{-2}$). The horizontal dashed (green) line marks the value of the chemical potential. The location of the peak for the upper branch Goldstone mode is explicitly plotted (red). Its fit to a linear dispersion is plotted in Fig. 2.

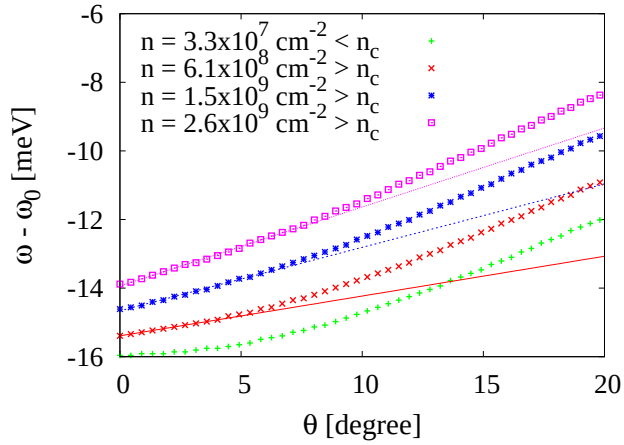

FIG. 2: Dispersion of the lower polariton at a density $n = 3 \times 10^7 \mathrm{cm}^{-2}$ (green) and dispersion of the upper branch of the Goldstone mode at $n = 6.1 \times 10^8 \mathrm{cm}^{-2}$ (red), $n = 1.51 \times 10^9 \mathrm{cm}^{-2}$ (blue), and $n = 2.59 \times 10^9 \mathrm{cm}^{-2}$ (magenta), for $T = 19$K and a detuning $\delta = +6$meV. The fits to a linear dispersion of the Goldstone modes are explicitly shown. Note that the shift in energy of the emission at zero momentum, which can be compared to the experimental one, is for the four curves respectively $\delta E = 0.01$meV, $\delta E = 0.55$meV, $\delta E = 1.30$meV, and $\delta E = 2.04$meV (the shift is measured with respect to the energy of the zero momentum lower polariton at extremely small densities).

both the linear behaviour of the collective modes at low momenta and the emission from below the chemical potential.

Nevertheless, the analysis of the linear behaviour of the Goldstone mode can give important information on the coherence properties of the condensate. In particular, the slope of the linear mode is the sound velocity of the condensate, c_s. As it will be shown in the next section, the sound velocity together with the temperature determines the lengthscale, the thermal length, for the decay of the spatial coherence.

In Fig. 2 we plot the upper branch of the Goldstone mode, obtained from evaluating the locations of the corresponding peaks as shown in Fig. 1, for increasing values of the polariton density n ranging from the non-condensed to the condensed regime. As shown in the picture, the extension of the linear behaviour grows with increasing density up to approximately 8° at the highest density considered. At the same time, the slope of the linear mode and therefore the sound velocity increases with increasing density.

B. Condensate emission — decay of spatial and temporal coherence

In the condensed state, because there is no restoring force for global phase fluctuations, the amplitude of phase fluctuations at low momenta can be large. However, there is a restoring force for amplitude fluctuations, and so except near the transition, it is valid to assume these to be small. Taking the phase fluctuations to all orders and the amplitude fluctuations to second order, one can calculate the first order coherence function:

$$g^{(1)}(t; \mathbf{r}) = [1 + \mathcal{O}(1/\rho_0)] \exp[-f(t, \mathbf{r})] \ . \qquad (3)$$

In this expression, the terms of order $\mathcal{O}(1/\rho_\prime)$ arise from including density fluctuations, but are not relevant in describing the long distance behaviour. This form asymptotes to the well-known power law decay of correlations at large times and distances, for which:

$$f(t, \mathbf{r}) = \eta \log\left(\frac{\sqrt{c_s^2 t^2 + r^2}}{\beta c_s}\right) \ . \qquad (4)$$

Here, c_s is the velocity of the Goldstone mode, ρ_0 is the mean-field estimate of the condensate density and $\eta = m k_B T/(2\pi\rho_0)$. The logarithmic dependence on the spatial coordinate r reflects the expected BKT decay of correlations for a two-dimensional system. Note that since the asymptotic form of the spatial decay is power-law, and not exponential, there is strictly no characteristic lengthscale of the decay, so the coherence length is not a well defined quantity. However, there does exist a lengthscale — the thermal length — which describes the distances at which the long range asymptotic behaviour begins to be relevant; below this lengthscale, correlations

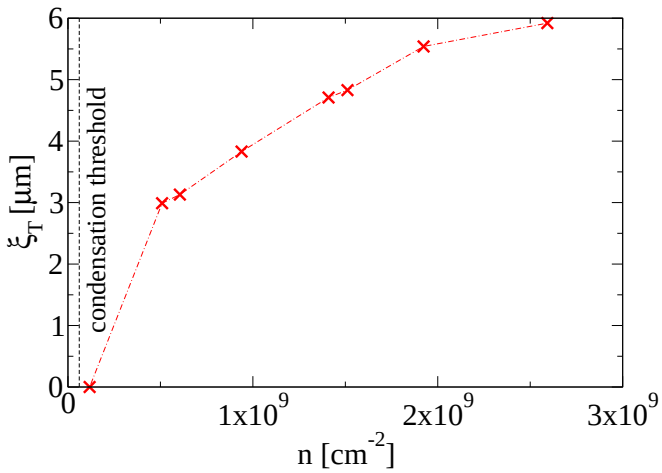

FIG. 3: Dependence of the thermal length ξ_T on the polariton density for $T = 19$K and a detuning $\delta = +6$meV.

are short range, and approximately independent of distance. This thermal length is given by:

$$\xi_T = 2\pi \frac{c_s}{k_B T} \ . \tag{5}$$

Substituting the values of the velocity of the Goldstone mode c_s determined in Section II A we obtain thermal lengths given by $\xi_T = 3.13\mu$m, 4.83μm, and 5.92μm respectively for polariton densities of $n = 6.1 \times 10^8 \text{cm}^{-2}$, $1.51 \times 10^9 \text{cm}^{-2}$, and $2.59 \times 10^9 \text{cm}^{-2}$ for $T = 19$K and a detuning $\delta = +6$meV. The dependence of the thermal length on the density is shown in Fig. 3. Experiments on coherence in CdTe reported a contrast of interference fringes up to 5% below the transition and up to 45% above the transition[6]. The 45% contrast has been measured up to a distance of roughly 6 μm after which the contrast drops to 30% up to a distance of roughly 12μm. Our estimates of the thermal length, of the order of 5μm, are consistent with these measurements. Unfortunately due to a very large spatial inhomogeneity of the condensate caused by large photonic disorder it was not possible in that experiment to examine a functional dependence of the decay of the correlation as a function of the distance. Spatial coherence has also been recently measured in GaAs systems[8]; such systems appear to show less spatial inhomogeneity, and so might allow fuller investigation of the decay of correlations at long distances. However, the data presented in Ref.[8] shows measurements of $g^{(1)}(0;\mathbf{r})$ at only six different separations, ranging between 1.3μm and 8μm. According to the analysis in that paper, the data are adequately described over that range by modelling the system as a degenerate Bose gas, without considering any changes to the dispersion of the bosons. Such a model is in effect a model of non-interacting Bosons, and so does not describe power law decay of correlations.

III. INFLUENCE OF PUMP, DECAY AND FINITE SIZE ON COHERENCE PROPERTIES

Since the effects of pump and decay in the polariton system are large compared to other relevant energy scales, such as temperature (one can, e.g., compare the homogeneous linewidth of polaritons, of roughly 1meV with the characteristic temperature $\sim$ 20K$\sim$ 1.7meV), we expect pump and decay to modify the coherence properties of the polariton condensate. We have addressed these issues by looking at the spontaneous condensation for a system, coupled to external baths, representing the pumping and decay mechanisms[14,15]. We have shown that, even when the polariton system is characterised by a thermal distribution, the presence of pumping and decay significantly modify the spectra of collective excitations. In particular, the low energy phase modes become diffusive at small momenta[14,15,17,18], leading to correlation functions — and thus condensate line-shape — that differ both from an isolated equilibrium BEC and from those for phase diffusion of a single laser mode. Here we give estimates of the size of the diffusive region for conditions close to those of the CdTe experiments.

A. Collective modes of the polariton condensate in presence of pump and decay

In the normal state the fluctuation spectrum shows the usual polariton branches, which are now also homogeneously broadened due to pumping and decay. In the condensed state, however, the collective modes have the following energy ω vs. momentum p form:

$$\omega = -ix \pm i\sqrt{x^2 - c_s^2 p^2} \ , \tag{6}$$

and are thus diffusive, rather than dispersive for $p \leq x/c_s$. Here, the parameter x is a non-linear function of the pumping and decay strength and determines the linewidth of the Goldstone mode. Similarly to an equilibrium picture, the structure of the collective modes will be reflected in the PL which is a product of the spectral weight and the occupation function. In Figure 4 we plot the PL spectra for the parameters characterising the recent experiments on CdTe[6,13]. It can be seen that in its low frequency and momentum part, the main feature of the spectrum is a flat region followed by a dispersive mode which then approaches the LP spectrum. As in the closed system, the coupling of particle- and hole-like bosonic excitations means that in the condensed state, the same mode structure can also be seen below the chemical potential. The spectral weight of this mode is however much weaker and so it is less visible in the luminescence in Fig. 4. Our numerical analysis shows that the range of the flat region depends mainly on the photon decay rate; but also depends weakly on the pump parameter γ such that the flat region should increase slightly with increasing pump power which is consistent with the experiment[20]. For the photon decay rate of 1ps

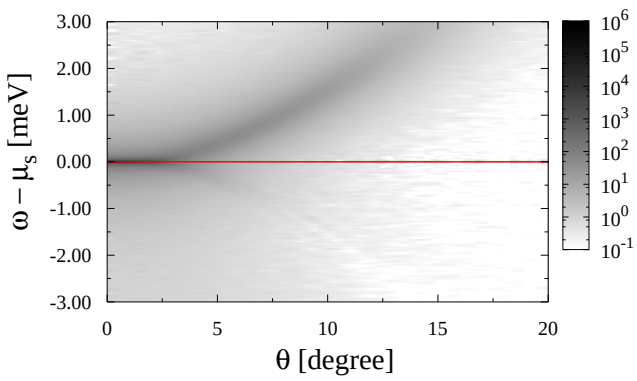

FIG. 4: Condensed luminescence spectra for the photon decay rate of 1ps ($\sim$ 0.49meV) and the parameter γ, representing the coupling strength to the pumping baths, γ=1.3meV. The frequency is shown with respect to the condensate frequency. The flat region is around 3 degrees.

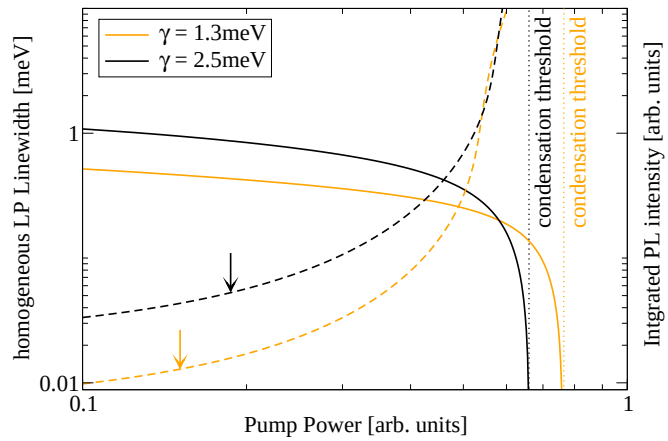

FIG. 5: Calculated homogeneous linewidth of the zero momentum lower polariton (solid line) and the integrated zero momentum PL intensity as a function of the pump intensity for two different dephasing parameters γ. The decay rate of the photon is determined from the homogeneous photon linewidth, measured to be around 1meV. The threshold for non-linear emission is explicitly shown.

($\sim$ 0.49meV) the size of the flat region extends up to around 5 degrees (depending on the coupling strength γ). There is also an alternative explanation that the observed flattening above the condensation transition is mainly due to the finite size effects[21]. Note that since the size of the flat region here is of similar order to the range over which the Goldstone mode is linear (see Figure 4), it is therefore possible that, at least close to the transition, the dispersion will cross directly from diffusive to quadratic, without a linear part.

B. Decay of temporal coherence

Similarly to an equilibrium picture, in order to examine the coherence properties of a condensed system, one needs to determine the field-field correlation functions including the phase fluctuations to all orders and to determine the analogue of expression (3) for a dissipative system. This approach has several advantages. Firstly it naturally includes both condensate and non-condensate luminescence in the same formalism, and (in the finite system) provides a linewidth for the condensed part. Secondly it recovers the correct power-law behaviour of occupation of modes in momentum space when integrated over frequencies. It has been shown[14,15] that for the infinite system with pump and decay the power-law which governs the decay of correlations in a 2D system changes to:

$$f(t,\mathbf{r}) \simeq \begin{cases} \dfrac{\eta'}{2}\log\dfrac{c_s^2 t}{x\xi_c^2} & \text{if } r\simeq 0,\ t\to\infty, \\ \eta'\log\dfrac{r}{\xi_c} & \text{if } r\to\infty,\ t\simeq 0. \end{cases} , \qquad (7)$$

where η', in distinction to η in Eq. (4), depends on x as well as temperature and condensate density, and ξ_c is a characteristic length scale for the non-equilibrium occupation function of polaritons, given by $\xi_c \propto c_s/E$, where E is a characteristic energy scale of the polaritons' distribution. Thus, there is still power-law decay, but due to pumping and decay the powers for temporal and spatial decay do not match. In the case of systems with strong pumping and decay, but where the distribution function is close to thermal, as in the recent experiments on CdTe[6], then $E \simeq k_B T$ and so

$$\xi_c = 2\pi\frac{c_s}{k_B T} \equiv \xi_T \ . \qquad (8)$$

Therefore, if the system, despite the presence of pump and decay, is able to thermalize, the thermal length is not strongly affected by the presence of pump and decay and its expression coincides with that of a closed system (5).

In order to understand the temporal coherence measurements[6] which show exponential decay, it turns out to be necessary to address the influence of finite size on the expression (3). A detailed analysis of this can be found in reference[15]. Summarising, in the finite condensed system the energy level spacing is given by $\Delta_\phi = c_s/R$ [note this differs from the single particle level spacing relevant for the uncondensed regime $\Delta_{\text{s.p.}} = 1/(2mR^2)$]. With this level spacing it has been shown[15] that the function which controls the decay of coherence can be approximately written as

$$f(t,\mathbf{r}=0) \propto \frac{1}{x}\left[\frac{t}{2x} + \frac{1}{\Delta_\phi^2}\log\left((k_B T)^2\frac{t}{x}\right)\right] \ . \qquad (9)$$

In this expression, we have used the assumption of a thermal distribution to write $k_B T$ for the high energy cutoff

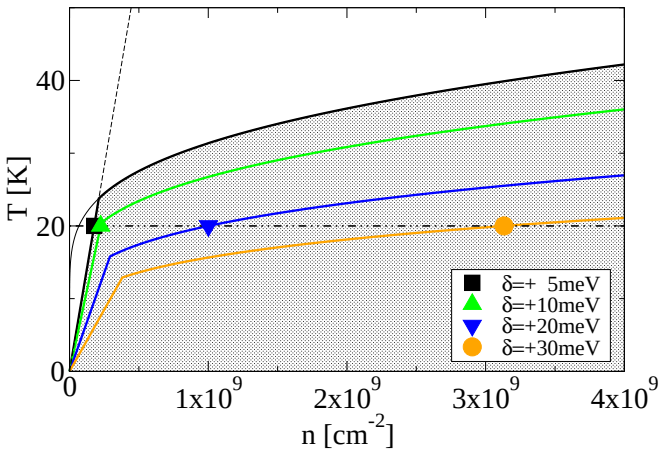

FIG. 6: Dependence of the polariton phase diagram on the detuning δ of the exciton mode below the bottom of the photon band. By fixing the polariton effective temperature at around 20K, the transition to the condensed phase (symbols) moves from the linear regime of the phase diagram to the regime where the boundary is determined by the long-range nature of the polariton-polariton interaction.

c_s/ξ_c as in Eq. (8). The first term, which dominates at large times, gives exponential decay of correlations whereas the second term gives the power-law decay characteristic for infinite 2D systems. The relative importance of these two terms depends on the system size and temperature (i.e how deep the system is into the condensed regime). If the system is large or is close to the phase boundary i.e where $k_BT \gg \Delta_\phi = c_s/R$ the second term (i.e power-law decay) dominates at short times and it crosses to exponential decay only at later times. Rearranging this condition it translates to $R \gg 2\pi c_s/k_BT = \xi_T$ which says that the system size is much larger than the thermal length. However if the system is small or deep inside the condensed region and so $k_BT \ll \Delta_\phi = c_s/R$ the phase fluctuations associated with 2D nature of the condensate are frozen out and the first term dominates giving an exponential decay at all times. This conditions translates to $R \ll 2\pi c_s/k_BT = \xi_T$. Thus spatial coherence over the whole system size implies the exponential decay of temporal coherence (however not vice-versa).

C. Linewidth in the normal state

In order to determine the homogeneous contribution to the polariton linewidth, i.e. that part due to pumping and decay as opposed to the linewidth resulting from structural disorder, we must explicitly consider an open system with incoherent pumping and decay of photons. Here, we focus only on the homogeneous linewidth of the normal state on approaching the transition. Following Refs.[14,15], the pumping process is described by two parameters: The occupation of the pumping bath which describes the pumping intensity, and the coupling constant γ between the system and the pumping bath, which gives rise to dephasing. Figure 5 shows the LP linewidth (solid lines) and the energy integrated zero momentum PL intensity (dashed lines) as a function of the pumping strength for two different values of γ. In both cases, the curves are plotted up to the pump power value corresponding to condensation.

It can clearly be seen that, at pumping powers below the phase transition, the intensity of photoluminescence already starts to increase non-linearly. Such non-linear effects in advance of the condensation transition are not surprising, since a second-order phase transition is associated with divergent susceptibilities. In addition, the homogeneous linewidth decreases as one approaches the transition, as the gain due to pumping balances the loss due to decay. Therefore, the pump power at which a minimum of linewidth is observed, which coincides with the appearance of temporal coherence, may provide a better indication of the phase boundary than is provided by the maximum nonlinearity of the photoluminescence, i.e. the threshold condition.

IV. EXCITON PHOTON DETUNING

In this last section we discuss some aspects of the polariton phase diagram and the possibility of experimentally exploring different parts of it. As already mentioned in the introduction, there has been a recent investigation[13] of the direct comparison between experimental and theoretical phase boundaries for condensation of polaritons in a CdTe microcavity. This work has shown that the current experimental data for the phase boundary lie close to the crossover between a BKT transition of structureless bosons (low density part of the diagram shown in Fig. 6) and a regime where instead the phase boundary is characterised by the long-range nature of the polariton-polariton interaction and where therefore the composite nature of polaritons matters (a region where the dependence of the critical temperature on the density is slower then linear). Those results therefore suggest that polariton condensation departs from the weakly interacting boson picture.

In that experiment[13], however, it has proven particularly difficult to change substantially the effective temperature of polaritons by changing that of the lattice (i.e. the cryostat temperature): Because of the short polariton lifetime, the polariton temperature is decoupled from that of the lattice. It has therefore not been possible to explore parts of the phase diagram other than the crossover region by means of changing temperature. However, if the effective temperature does not change much, then one can shift the boundary from the structureless boson to the long-range interaction part of the phase diagram, by changing the detuning between the photon and the exciton (see Fig. 6).

The change to the phase boundary due to detuning

can be simply explained in the low density (weakly interacting Bose gas) limit, as the increase of the polariton effective mass with the detuning — in this regime one can show that $k_B T_c \propto n/m_{\rm pol}$ and neglecting exciton dispersion one may write, $m_{\rm pol} = 2m_{\rm photon}/[1-\delta/\sqrt{\delta^2+\Omega_R^2}]$, in which $m_{\rm photon}$ is the photon mass, and Ω_R the Rabi-splitting at zero detuning, and zero-density. In the high density, long-range interaction part of the phase diagram the decrease of the critical temperature with the detuning at a fixed density is due to two mechanisms: a loss of coherence in the system as, when increasing the detuning, the lower polariton becomes less photon-like; and the decrease of the effective exciton-photon coupling, which controls the critical temperature at higher densities. In Fig. 6 we show that in order to see a significant move of the condensate threshold from the low-density to the high-density part of the phase diagram, one has to go at least to positive detunings larger that 20meV. Unfortunately, this has proven to be a challenge experimentally, and current experiments in CdTe allow one to reach a maximum detuning of roughly 12meV[13].

V. CONCLUSIONS

To summarise, we have analysed the spatial and temporal coherence properties of a two-dimensional, finite, and decaying condensate with parameters tailored to the recent experiments on CdTe microcavities. We have shown that the theoretical estimate of the thermal length (over which there is no decay of coherence) of up to 6 μm, and the exponential decay of temporal coherence are consistent with those found in experiment. We have also estimated the size of the dispersionless (flat) region in the PL — a manifestation of the diffusive nature of the Goldstone mode — to be around 5 degrees. This result suggests that the flattening of the polariton dispersion above the transition may be attributed to the dispersionless nature of the Goldstone mode. Since at current experimental conditions the linear part of the dispersion is of a similar size to the diffusive part it is likely that the flat region will cross directly to the quadratic dispersion and that the linear part will not be visible. In order to see linear dispersion, it would be necessary to decrease the size of the diffusive regime, which would require an improvement in the quality of the cavity mirrors. Finally we analyse the dependence of the phase diagram on exciton-photon detuning and suggest that going to higher positive detunings might provide a means of exploring different parts of the phase diagram.

Acknowledgements We are grateful to L. S. Dang and J. Kasprzak for stimulating discussions. F.M.M. and M.H.S. would like to acknowledge financial support from EPSRC. J.K. would like to acknowledge financial support from Pembroke College Cambridge.

[1] L. S. Dang, D. Heger, R. André, F. Bœuf, and R. Romestain, Phys. Rev. Lett. **81**, 3920 (1998).
[2] J. Keeling, F. M. Marchetti, M. H. Szymańska, and P. B. Littlewood, Semicond. Sci. and Technol. pp. R1–R26 (2007).
[3] P. R. Eastham and P. B. Littlewood, Solid State Commun. **116**, 357 (2000).
[4] A. Kavokin, G. Malpuech, and F. P. Laussy, Phys. Lett. A **306**, 187 (2003).
[5] J. Keeling, P. R. Eastham, M. H. Szymanska, and P. B. Littlewood, Phys. Rev. Lett. **93**, 226403 (2004).
[6] J. Kasprzak, M. Richard, S. Kundermann, A. Baas, P. Jeambrun, J. M. J. Keeling, F. M. Marchetti, M. H. Szymanska, R. Andre, J. L. Staehli, et al., Nature **443**, 409 (2006).
[7] H. Deng, D. Press, S. Götzinger, G. S. Solomon, R. Hey, K. H. Ploog, and Y. Yamamoto, Phys. Rev. Lett. **97**, 146402 (2006).
[8] H. Deng, G. S. Solomon, R. Hey, K. H. Ploog, and Y. Yamamoto, **99**, 126403 (2007).
[9] R. Balili, V. Hartwell, D. Snoke, L. Pfeiffer, and K. West, Science **316**, 1007 (2007).
[10] S. Christopoulos, G. Baldassarri, P. G. Lagoudakis, A. Grundy, A. V. Kavokin, J. J. Baumberg, G. Christmann, R. Butté, E. Feltin, J.-F. Carlin, et al., Phys. Rev. Lett. **98** (2007).
[11] G. Malpuech, Y. G. Rubo, F. P. Laussy, P. Bigenwald, and A. V. Kavokin, Semicond. Sci. and Technol. **18**, S395 (2003).
[12] F. M. Marchetti, J. Keeling, M. H. Szymańska, and P. B. Littlewood, Phys. Rev. Lett. **96**, 066405 (2006).
[13] F. M. Marchetti, M. H. Szymańska, J. Keeling, J. Kasprzak, R. André, L. S. Dang, and P. B. Littlewood, Phys. Rev. B **77**, 235313 (2007).
[14] M. H. Szymańska, J. Keeling, and P. B. Littlewood, Phys. Rev. Lett. **96**, 230602 (2006).
[15] M. H. Szymańska, J. Keeling, and P. B. Littlewood, Phys. Rev. B **75** (2007).
[16] J. Keeling, P. R. Eastham, M. H. Szymanska, and P. B. Littlewood, Phys. Rev. B **72**, 115320 (2005).
[17] M. Wouters and I. Carusotto, Phys. Rev. B **74**, 245316 (2006).
[18] M. Wouters and I. Carusotto, Phys. Rev. A **76**, 043807 (2007).
[19] F. M. Marchetti, J. Keeling, M. H. Szymańska, and P. B. Littlewood, Phys. Rev. B **76**, 115326 (2007).
[20] J. Kasprzak, Ph.D. thesis, Universite Joseph Fourier, Grenoble (2006).
[21] J. Kasprzak, R. André, L. S. Dang, I. A. Shelykh, A. V. Kavokin, Y. G. Rubo, K. V. Kavokin, and G. Malpuech, Phys. Rev. B **75**, 045326 (2007).